Journal Pre-proofs

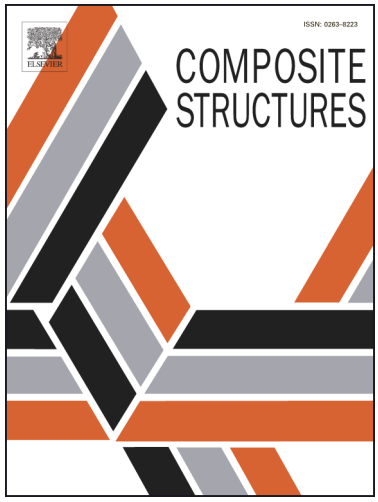

Compressive behaviour of concrete-filled carbon fiber-reinforced polymer steel composite tube columns made of high performance concrete

Krzysztof Ostrowski, Mateusz Dudek, Łukasz Sadowski

PII: S0263-8223(19)32708-4
DOI: https://doi.org/10.1016/j.compstruct.2019.111668
Reference: COST 111668

To appear in: *Composite Structures*

Received Date: 17 July 2019
Revised Date: 1 November 2019
Accepted Date: 3 November 2019

Please cite this article as: Ostrowski, K., Dudek, M., Sadowski, L., Compressive behaviour of concrete-filled carbon fiber-reinforced polymer steel composite tube columns made of high performance concrete, *Composite Structures* (2019), doi: https://doi.org/10.1016/j.compstruct.2019.111668

Compressive behaviour of concrete-filled carbon fiber-reinforced polymer steel composite tube columns made of high performance concrete

Krzysztof Ostrowski[1, ✉], Mateusz Dudek[2] , Łukasz Sadowski[3]

[1] Institute of Building Materials and Structures, Cracow University of Technology, 24 Warszawska Str. 31-155 Cracow, Poland

[2] Strata Mechanics Research Institute, Polish Academy of Sciences, ul. Reymonta 27, 30-059, Cracow, Poland

[3] Faculty of Civil Engineering, Wroclaw University of Science Technology, Wybrzeże Wyspiańskiego 27, 50-370 Wroclaw, Poland

✉: krzysztof.ostrowski.1@pk.edu.pl

Abstract:

The confinement of concrete-filled steel columns (CFT) with carbon fiber-reinforced polymer (CFRP) has been extensively studied in recent decades due to their significant applications for the strengthening purposes or construction of composite structures. A CFT column consists of a steel tube and inner-filled concrete, where the steel tube is used as a form and confinement of the concrete, with the concrete being the core that prevents buckling of the tube. Due to the development of concrete technology, high performance concrete (HPC) is increasingly used as the internal material of CFT. However, CFT columns are susceptible to local buckling and constant confining stress after yielding of the steel tube. This is why concrete-filled carbon fiber-reinforced polymer steel composite tubes (CFCT) have been considered. The key parameter, which determines load-carrying capacity, and axial and transverse deformation is the number of CFRP layers. The test results showed that local buckling of the steel tube can be effectively eliminated and that the compressive strength of CFCT is enhanced by the external confinement. It has been shown that the stress-strain characteristic depends on confinement pressure. This paper also discusses damage patterns and presents analysis of limit load capacity based on both laboratory experiments and numerical calculations.

Keywords: composite column, fibre-reinforced polymer material, high performance concrete, mechanical properties, numerical analysis, finite element method

Nomenclature

D - diameter of the specimen [mm],

E_c – elasticity modulus of the high performance concrete [GPa],

E_{er1} - modulus of elasticity in flexural of the epoxy resin [GPa],

E_{er2} - modulus of elasticity in tensile of the epoxy resin [GPa],

E_f -elastic modulus of the carbon fiber-reinforced polymer [GPa],

E_s-elasticity modules of the steel tube and steel section [GPa],

F_{er} - tensile strength of the epoxy resin [MPa],

f_{cc1}- nominal axial stresses at the beginning of the transitional zone [MPa],

f_{cc2}- nominal axial stresses at the end of the transitional zone [MPa],

f_{ccu}- ultimate nominal axial stresses [MPa],

f_{frp}-hoop tension strength of the carbon fiber-reinforced polymer jackets [MPa],

f_u-ultimate strength of the steel tube and steel section [MPa],

f_y -yield strength of the steel section and steel tube [MPa],

H - height of the specimen [mm],

s_{frp}-density of the carbon fiber-reinforced polymer jacket [g/m^2],

t_{frp}- thickness of 1 layer of the carbon fiber-reinforced polymer jacket [mm],

t_s- thickness of the steel tube [mm],

δ_{frp}-elongation percentage of the carbon fiber-reinforced polymer jacket [%],

ρ_{er} - density of the epoxy resin [kg/dm^3],

δ_{er} - elongation at break of the epoxy resin [%],

δ_s-elongation percentage of the steel tube and steel section [%],

ε_{cF}- plastic strain at failure [-],

ν_c – Poisson ratio of the high performance concrete [-],

ν_f – Poisson ratio of the carbon fiber-reinforced polymer [-],

ν_s- Poisson ratio of the steel [-],

σ_{cT}- cracking failure stress [MPa]

σ_{cU}- crushing failure stress of the high performance concrete [MPa],

σ_{cY} – yield stress of the high performance concrete [MPa],

σ_{sU} – ultimate strength of the steel [MPa],

σ_{sY} – yield stress of the steel [MPa],

ε_{cc1}- nominal axial strains at the beginning of the transitional zone [-],

ε_{cc2}- nominal axial strains at the end of the transitional zone [-],

ε_{ccu}- ultimate nominal axial strains [-].

1. Introduction

Concrete-filled steel tube (CFT) columns have been studied and frequently applied in civil engineering and construction. CFT columns have the advantages of the synergy of steel and concrete. However, these elements are unfortunately susceptible to local buckling, poor durability and the constant confining stress after the yielding of steel tubes [1-3]. Composite structures can be seen to be much more effective [4]. In recent years, carbon fibre reinforced polymer (CFRP) composite structures have found an all-embracing appliance in civil engineering [5]. With the recent advances in the technology of composite materials, CFRP has initiated a new level in the area of civil engineering to repair and retrofit existing supporting elements or to design new infrastructures [6]. CFRP has a high strength, Young's modulus, and strength-to-weight ratio, as well as resistance to aggressive environments and good fatigue and installation properties. An CFRP jacket is a kind of orthotropic material that is suitable for encircling the concrete column, which is in contrast to the anisotropy of concrete and the isotropy of steel. CFRP confinements are based mostly on epoxy resins and allow for a composite to be put together with steel, concrete and wood [7].

It has been proven many times that the outer reinforcement of CFRP increases the effectiveness of retrofitting and/or repairing concrete elements. Researchers have shown that using CFRP in the case of special concretes such as normal-performance fibre reinforced concrete could improve the bearing capacity of short concrete columns and change their post-peak characteristic [8]. Lim and Ozbakkaloglu showed that the failure energy of CFRP depends on the strength of the concrete [9]. Jiang et. al [10], in order to determine the behaviour of CFRP confined columns made with ultrahigh-strength concrete, analysed specimens reinforced with glass fibre reinforced polymer material. In this research, a significant strengthening of specimens was observed. Moreover, in part of the specimens, delamination of the GFRP in the overlapping zone was noted.

In recent years, the stress-strain performance of high strength concrete confined with CFRP material was determined for elements with a circular and square shape. As a result, an increased efficiency of the outer confinement in circular shape specimens occurred [11]. Kamiński and Trapko proposed a new strengthening solution for structural CFRP elements in reinforced concrete elements where the CFRP was stuck in selected areas [12]. The impact of E-glass and carbon CFRP on the behaviour of five classes of concrete strength (since 24 to 170 MPa) was analysed by Berthet et al. [13]. Park et. al. [14] used narrow CFRP strips in many combinations to reinforce concrete columns with a compressive strength equal to 20.72 and 26.08 MPa. In general, current literature contains a lot of surveys that involve the strengthening of concrete by CFRP in varied types of specimens such as classic columns [15], elements with CFRP material in concrete grooves [16], and concrete columns under eccentric load [17]. The development of CFRP techniques could also be observed in the case of beam structures. Zaki et al. [18] proposed CFRP fibre anchors and dowels as the reinforcement in T-

shape beams. Zhang et al. [19] proposed the use of CFRP stirrups in the reinforcement of concrete beams produced of reinforced and recycled aggregate concrete.

The most commonly used matrix system uses epoxy resins. Epoxy resins have some disadvantages, such as their weak performance in high temperature conditions, fairly high cost, lack of vapour permeability, hazards for manual workers, and the difficulty in assessing the post-earthquake damage of reinforced concrete behind composite jackets [20]. The biggest drawback can be seen to be the loose adhesive properties of epoxy resins upon reaching glass transition temperature (over 50 °C). This is why the fibre reinforced cementitious matrix is increasingly used when reinforcing concrete structures. According to the performed studies, the efficiency of the bond between a concrete surface and cement-based composites in confined mode is acceptable [21]. In the case of using fibre reinforced cementitious matrix when reinforcing a concrete structure, the crucial parameter that has an influence on the load-carrying effectiveness is a properly prepared concrete surface. This aspect will be studied by the authors in future research. Unfortunately, fibre reinforced cementitious matrix is not suitable for reinforcing steel elements.

When considering the above, concrete-filled carbon fiber-reinforced polymer steel composite tube columns have been contemplated as an alternative structure for new infrastructure in civil engineering due to their steel-free construction and corrosion resistance. As has been shown many times, concrete-filled carbon fiber-reinforced polymer steel composite tube columns show great performance during compression tests [22-24]. Fam et al. [25] and Zhu et al. [6] described the behaviour of concrete-filled carbon fiber-reinforced polymer steel composite tube columns in combination with axial compression and lateral loading. Most drawbacks of concrete-filled carbon fiber-reinforced polymer steel composite tube columns include the low stiffness of CFRP tubes and unsatisfactory rigidity, which is necessary to distribute loading on a construction. It has been proven that combining materials with different properties can give beneficial results. The compressive behaviour of composite columns with miscellaneous parameters was investigated many times, and analytical and numerical models were expanded to assess the behaviour of composite columns for different slenderness ratios [27-29]. Usually, concrete-filled carbon fiber-reinforced polymer steel composite tube columns were made using normal strength concrete. However, according to the authors' knowledge, there is lack of research on the compressive behaviour of concrete-filled carbon fiber-reinforced polymer steel composite tubes (CFCT).

In 2005, Xiao et al. proposed CFRP as a supplementary material for CFT columns in order to control the local buckling of the steel tube and to provide the quasiplastic range of work of the CFT [30]. The obtained axial compression test results showed that the additional CFRP reinforcement provides great seismic performance. Circular CFT columns reinforced with CFRP have been studied many times in research [31-33]. Researchers proved that the type, stiffness and number of layers of CFRP

confinement and the thickness of steel tube have a significant impact on the load-carrying capacity and the ductility of CFT columns. Sundarraja and Prabhu examined square CFT columns reinforced by CFRP. These experimental results showed that the confining pressure to the CFT columns was increased when using CFRP. When compared to CFT columns, columns reinforced by CFRP have a higher ultimate load and larger deformation [34,35]. Using analytical methods, many theoretical models that describe the load capacity behaviour of concrete-filled carbon fiber-reinforced polymer steel composite tubes (CFCT) columns were proposed [36-38].

Considering the above, the main goal of this article is to experimentally investigate the compressive behaviour of steel tubes filled with high performance concrete confined by a various number of CFRP layers. The following questions remain unanswered. Does the efficiency of reinforcing depend on the number of layers? How do the stress–strain curves of the confined specimens appear? Is the stress-strain behaviour of CFRP-confined elements similar to those reported in the literature? Additionally, these answers will be supported by numerical analysis that is carried out based on the average values of the physical-mechanical parameters obtained from laboratory tests.

2. Research significance

The novelty of this research focuses on the investigation of the load-carrying capacity of concrete-filled carbon fiber-reinforced polymer steel composite tubes (CFCT) columns manufactured using high performance concrete (HPC). Moreover, HPC was used in this research as the internal material, which has not often been analyzed by other researchers. Finally, a composite structure consisting of HPC, steel, and carbon fibres reinforced by epoxy resin may lead to a structure being obtained that has a high bearing capacity, is insusceptible to dynamic effects and is resistant to the effects of an aggressive environment.

3. Test program

3.1. Details of specimens

All specimens, depending on their type, were divided into 5 groups. The program involved testing on 21 samples: 3 steel pipes (SP), 3 concrete cores manufactured with high-performance concrete (HPC), 3 high-performance concrete cores reinforced with one layer of carbon fiber-reinforced polymer (HPC-CFRP), 3 concrete-filled steel columns (CFT) columns, and 9 concrete-filled carbon fiber-reinforced polymer steel composite tubes (CFCT) tubes reinforced with 1, 2 and 3 layers of CFRP (3 specimens of each type). The outer diameter in the case of the SP, CFT and CFCT columns refers to the outer diameter of the steel tube. The thickness of the CFRP was omitted. Details of the specimens are shown in Table 1.

Table 1. Details of test specimens

Type of the specimen	Specimen	Diameter of the specimen *D* [mm]	Height of the specimen *H* [mm]	Thickness of steel tube [mm]	Carbon fiber-reinforced polymer (CFRP) sheets	Number of specimen
Steel pipes (SP)	SP1 SP2 SP3	159	400	4.5	-	3
High-performance concrete (HPC)	HPC1 HPC2 HPC3	150	400	-	-	3
High-performance concrete cores reinforced by one layer of carbon fiber-reinforced polymer (HPC-CFRP)	HPC-CFRP1 HPC-CFRP2 HPC-CFRP3	150	400	-	1	3
Concrete-filled steel columns (CFT)	CFT1 CFT2 CFT3	159	400	4.5	-	3
Concrete-filled carbon fiber-reinforced polymer steel composite tube (CFCT)	CFCT1-1 CFCT1-2 CFCT1-3	159	400	4.5	1	3
	CFCT2-1 CFCT2-2 CFCT2-3				2	3
	CFCT3-1 CFCT3-2 CFCT3-3				3	3

3.2. Material properties

The high performance concrete (HPC) concrete used in this research was sourced from a local concrete supplier. The concrete used in the tests was prepared using Portland Cement type I 42.5R (Górażdże, Poland), a 0.4 water/cement ratio, SikaFume additive in fine-powder form based on silica fume technology, and superplasticiser Sikament FM6 (Sika Poland sp. z o. o., Warsaw, Poland) based on an aqueous solution of modified polycarboxylates. Separated diabase coarse aggregate (Krzeszowice, Poland) and fine aggregate (Brzegi, Poland) were used. The detailed mix designs for the concrete are given in Table 2. The average compressive strength of the 6 cubic specimens with dimensions of 150x150x150 mm was 86.5 MPa.

Table 2. Proportions of the mix used to make the high-performance concrete (HPC).

Cement [kg/m^3]	Fine Aggregate [kg/m^3]	Coarse Aggregate [kg/m^3]	Water [kg/m^3]	Sika Fume [kg/m^3]	Super-Plasticiser [kg/m^3]
500	650	1000	200	60	10

Steel tubes with an outer diameter of 159 mm and a length of 400 mm were used in the survey. The properties of the tubes are determined in Table 3.

Table 3. Selected properties of steel tubes.

Symbol and unit	fy [MPa]	E_s [GPa]	δ_s [%]	f_u [MPa]	t_s [mm]
Value	235	210	24	410	4

CFRP layers were chosen as the confinement due to the high performance of this material. Table 4 presents the main properties of the CFRP.

Table 4. Selected properties of carbon fibre reinforced polymer (CFRP)

Symbol and unit	f_{frp} [MPa]	E_f [GPa]	δ_{frp} [%]	s_{frp} [g/m^2]	t_{frp} [mm]
Value	4900	230	1.7	304	0.167

The epoxy resin Sikadur330, used for building structures, was adopted for gluing the CFRPs together and adhering the CFRP to the steel tube. The main parameters of the resin are shown in Table 5.

Table 5. Selected properties of epoxy resin.

Symbol and unit	f_{er} [MPa]	E_{er1} [GPa]	E_{er2} [GPa]	δ_{er} [%]	ρ_{er} [kg/dm^3]
Value	30	3.8	4.5	0.9	1.3±0.1

Note: Properties after 7 days at +23°C;

3.3. Specimen preparation

All the steel tubes were cut from the same material in order for the properties of the steel tubes for the different specimens to be the same. The ends of all the specimens were machined on a lathe to achieve a flat and vertical surface. The concrete mixture was made with the use of a concrete mixer, where all the components were mixed. Firstly, the coarse and fine aggregate were mixed for 60 seconds, then cement, silica fume and water with superplasticizer were added and mixed for 300 seconds. The time of the mixing process was relatively long due to the admixture content. In the case of the HPC, the effect of adding the superplasticizer could be observed after 3 to 5 minutes of mixing. This mixture was produced according to EN 206 [39]. The concrete was compacted two times during the filling of the forms - after filling half of the mold and again after concreting the entire sample. The surface of the steel pipes was grinded to remove rust and then cleaned using alcohol to obtain an adequate bond strength between the epoxy resin and steel. To ensure the appropriate bond strength in the case of the HPC-CFRP columns, the surface of the HPC was grinded. The concrete surface before preparation and after grinding is shown in Figure 1. The confined elements were wrapped with CFRP using epoxy resin Sikadur330 during the manual dry layup process. A ribbed roller was used to eliminate air and voids by rolling the surface of the fiber in the hoop direction during the lamination process. In all cases, the principal fibers were oriented perpendicular to the column axis, in a so-called 0° orientation. An overlapping zone of the confined specimens in each layer i.e. 150 mm, was provided. The age of the concrete specimens at the moment of testing was six weeks.

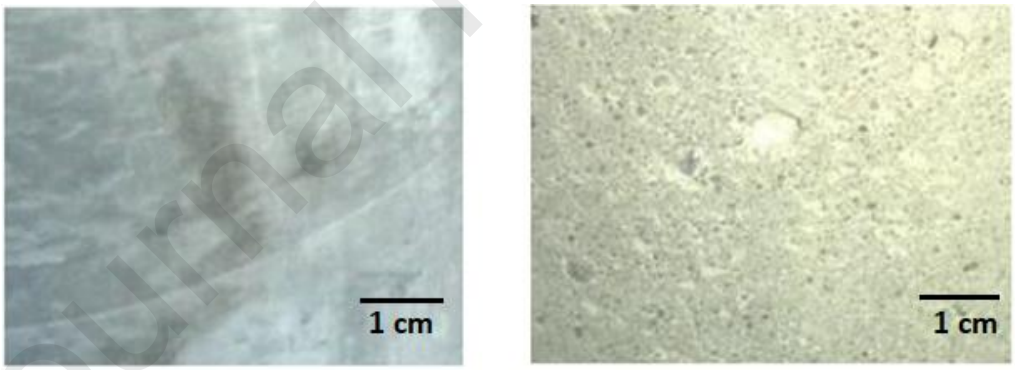

Figure 1. The optical views of the concrete surface before (left) and after the grinding process (right)

3.4. Instrumentation and loading conditions

The compression tests were carried using a 4600-kN capacity servo-controlled MTS Rock and Concrete Mechanics Testing System. The research was carried out at an air temperature of 20±1°C and humidity of 60±5%, with the constant axial strain rate of the samples in all of the experiments being approximately 3x10-5[s^{-1}]. The measurement of the axial force was carried out by means of a force transducer, while the displacements were measured by an extensometer. Radial and axial displacements were determined through the measurement of all of the specimens' dimension changes,

where the extensometer was mounted directly between the compression plates. The layout of the extensometer on the specimens is shown in Figure 2. The determination of compressive strength was determined according to EN 12390-3 [40].

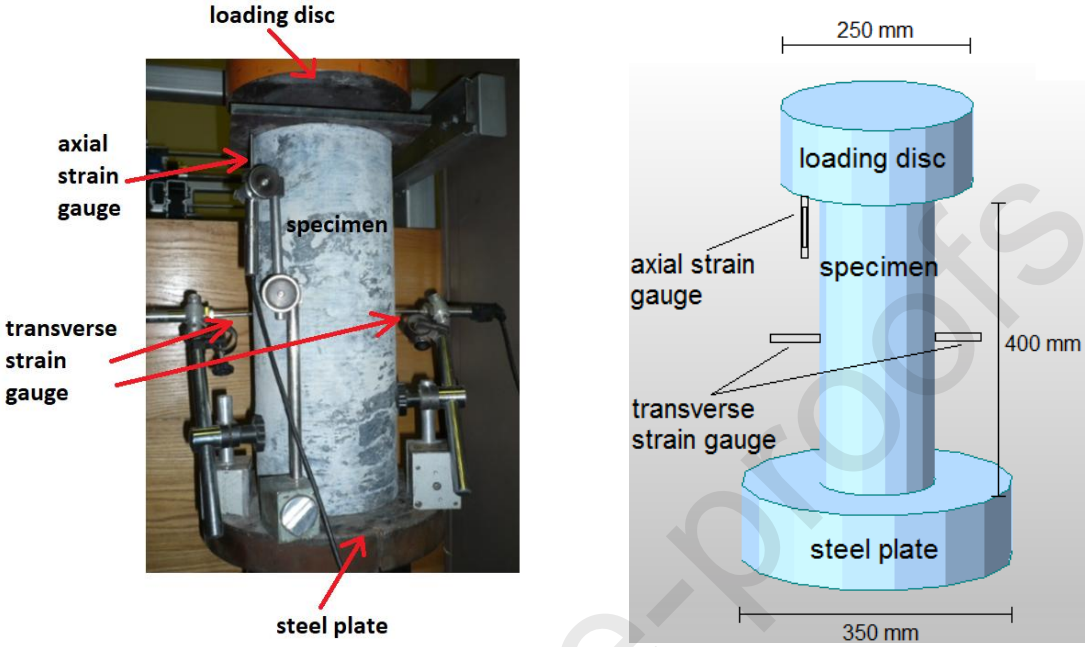

Figure 2. The tested specimen: view of the specimen (left) and scheme of the specimen (right).

3. Experimental results

3.1. Observed failure modes

The typical failure modes, representative for all the specimens, are shown in Figure 3. In the case of the HPC, formation of the cones on the border of the uniaxial and three dimensional state of stress was observed. This indicates that the samples were flawlessly processed. The failure of the HPC-CFRP columns occurred in a sudden and explosive way and was preceded by typical creeping sounds. The ringed rupture of the whole of the HPC-CFRP specimens (or localized in upper parts) is connected with a slight delamination of the CFRP layers from the concrete surface. This could be potentially caused by the localized effects of concrete shrinkage, as evaporation only occurs at the top surface. In the case of the concrete-filled steel columns (CFT) columns, in all cases there was a local buckling of the upper edge. This is connected with the plasticization of this area, and can be seen in Figure 3c. When analysing the concrete-filled carbon fiber-reinforced polymer steel composite tubes (CFCT) columns it can be noticed that the location of the rupture of the CFRP confinement depends on the number of layers. In the case of strengthening the specimen with one layer of CFRP, rupture of the reinforcement in the top half of the specimen can be observed (Figure 3d). With the increase of the number of reinforcing layers, the area of destruction of the reinforcement moves towards the middle part of the sample (as in the case of the reinforcement with 3 layers - Figure 3e). In reference to the

CFT and CFCT columns, a previous CFRP fracture, no local buckling, or any obvious dilation was observed in the specimens, and the deformation displayed was stable. All of the CFT and CFCT specimens exhibited a large deformation capacity. The bonding strength could not oppose the hoop tensile force produced by radial expansion once the CFRP fractured, and debonding failure occurred in conjunction with the CFRP fracture. It was observed that debonding failure does not occur before the fracture of CFRP.

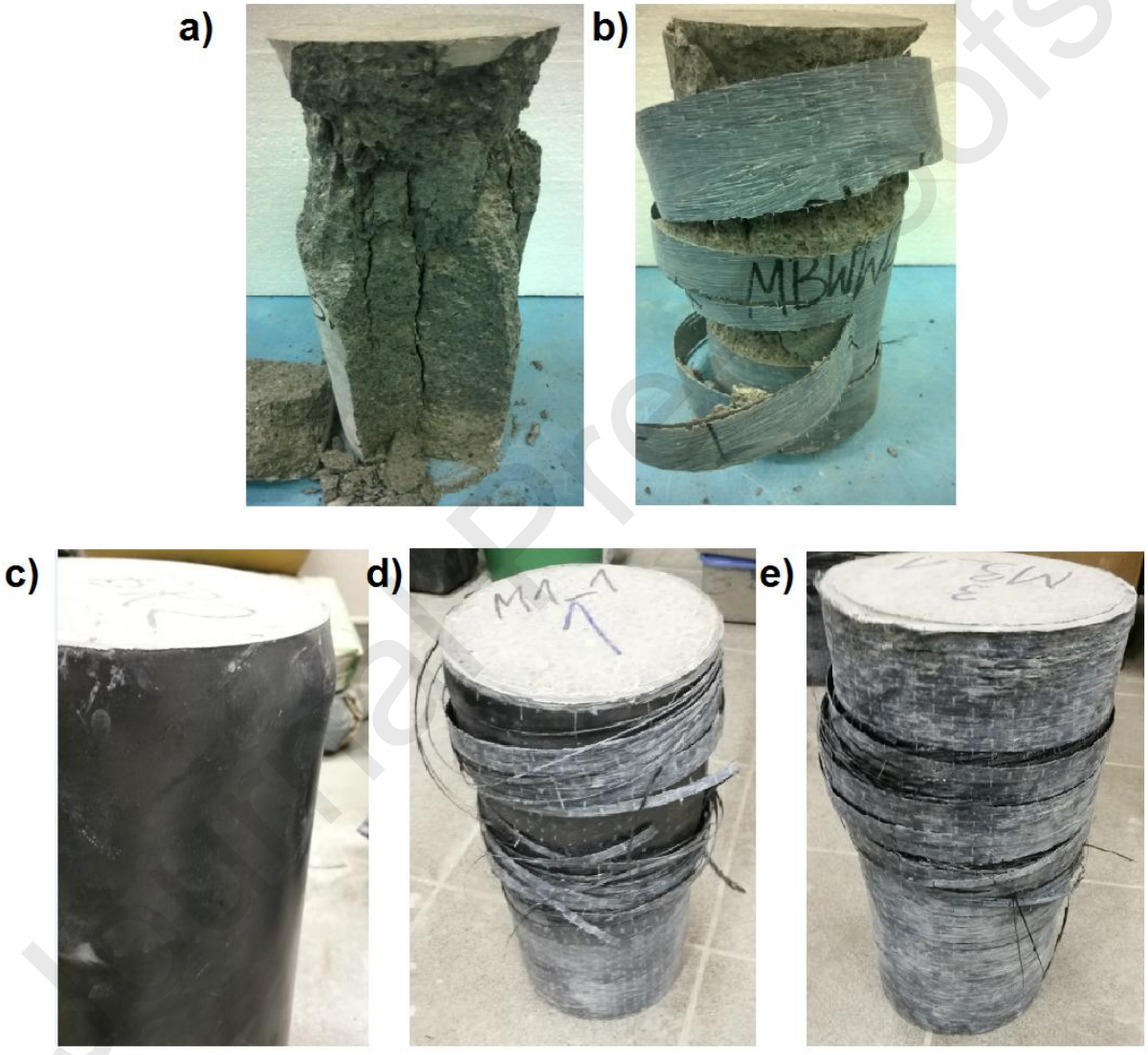

Figure 3. Typical failure modes of the tested specimens: a) concrete cone on the border of the uniaxial and three-dimensional state of stress, b) ringed rupture, c) local buckling on the top of the specimen, d) top half rupture, e) continuous rupture in the middle part of the specimen

3.2. Stress-strain relationship

Table 6 contains experimental values obtained from testing the specimens. The stress and strain values of the three points were obtained from the data measured from each specimen. The three key points were defined as: the beginning of the transitional zone (Point 1), the end of the transitional zone (Point 2), and the final of the second linear branch (ultimate). Figures 2 and 3 show the axial stress and strains for the specimens. The nominal axial stresses were calculated by dividing the axial loads by the total cross- sectional areas of the columns, and the small thickness of the CFRP was negligible in this calculation.

Table 6. Experimental values obtained from testing the specimens

Specimen	ε_{cc1} [-]	ε_{cc2} [-]	ε_{cu} [-]	f_{cc1} [MPa]	f_{cc2} [MPa]	f_{ccu} [MPa]
SP1	**-**	**-**	**18.10**	**-**	**-**	**294.33**
SP2	**-**	**-**	**17.20**	**-**	**-**	**300.22**
SP3	**-**	**-**	**13.24**	**-**	**-**	**283.99**
HPC1	**4.19**	**-**	**4.19**	**74.25**	**-**	**74.25**
HPC2	**4.79**	**-**	**4.79**	**57.36**	**-**	**57.36**
HPC3	**4.40**	**-**	**4.40**	**63.12**	**-**	**63.12**
HPC-CFRP1	**6.16**	**11.18**	**11.18**	**80.04**	**59.14**	**59.14**
HPC-CFRP2	**5.17**	**8.80**	**8.80**	**92.50**	**67.35**	**67.35**
HPC-CFRP3	**5.52**	**9.38**	**9.38**	**85.70**	**58.36**	**58.36**
CFT1	**7.26**	**11.65**	**24.32**	**101.46**	**90.32**	**80.27**
CFT2	**11.45**	**15.97**	**23.00**	**106.83**	**73.05**	**68.79**
CFT3	**11.89**	**16.27**	**25.66**	**106.55**	**80.68**	**70.88**
CFCT1-1	**12.88**	**22.66**	**25.88**	**120.41**	**88.84**	**87.94**
CFCT1-2	**14.72**	**19.64**	**26.00**	**114.00**	**82.94**	**75.10**
CFCT1-3	**13.21**	**19.38**	**25.40**	**112.51**	**80.08**	**74.97**
CFCT2-1	**21.76**	**25.96**	**39.90**	**139.98**	**103.16**	**83.70**
CFCT2-2	**21.50**	**27.81**	**37.59**	**147.71**	**90.88**	**81.00**
CFCT2-3	**20.83**	**30.41**	**33.87**	**136.60**	**85.03**	**84.78**
CFCT3-1	**20.80**	**22.50**	**34.00**	**143.51**	**96.28**	**92.28**
CFCT3-2	**30.56**	**32.53**	**41.47**	**178.87**	**109.96**	**91.04**
CFCT3-3	**20.42**	**26.62**	**35.00**	**150.15**	**116.06**	**103.66**

Figure 4 shows the axial stress-strain relationship for the SP, HPC and HPC-CFRP specimens. The average maximum stress of the steel pipes occurred at 292.85 MPa. The average compressive strength of the HPC is 64.91 MPa. Standard deviation in this case is 7.01 MPa. The average longitudinal and

transverse strains of the HPC at the time of destruction are 4.68 ‰ and 3.72‰, respectively. In the case of the HPC-CFRP columns, in reference to the HPC, an increase of the compressive strength and axial strain by 33% and 20% respectively at the moment of maximum load capacity was observed. The behaviour of the HPC-CFRP is close to linearly elastic until the maximum stress is obtained. After exceeding the load capacity, a step loss of stiffness occurred, which led to the destruction of the element.

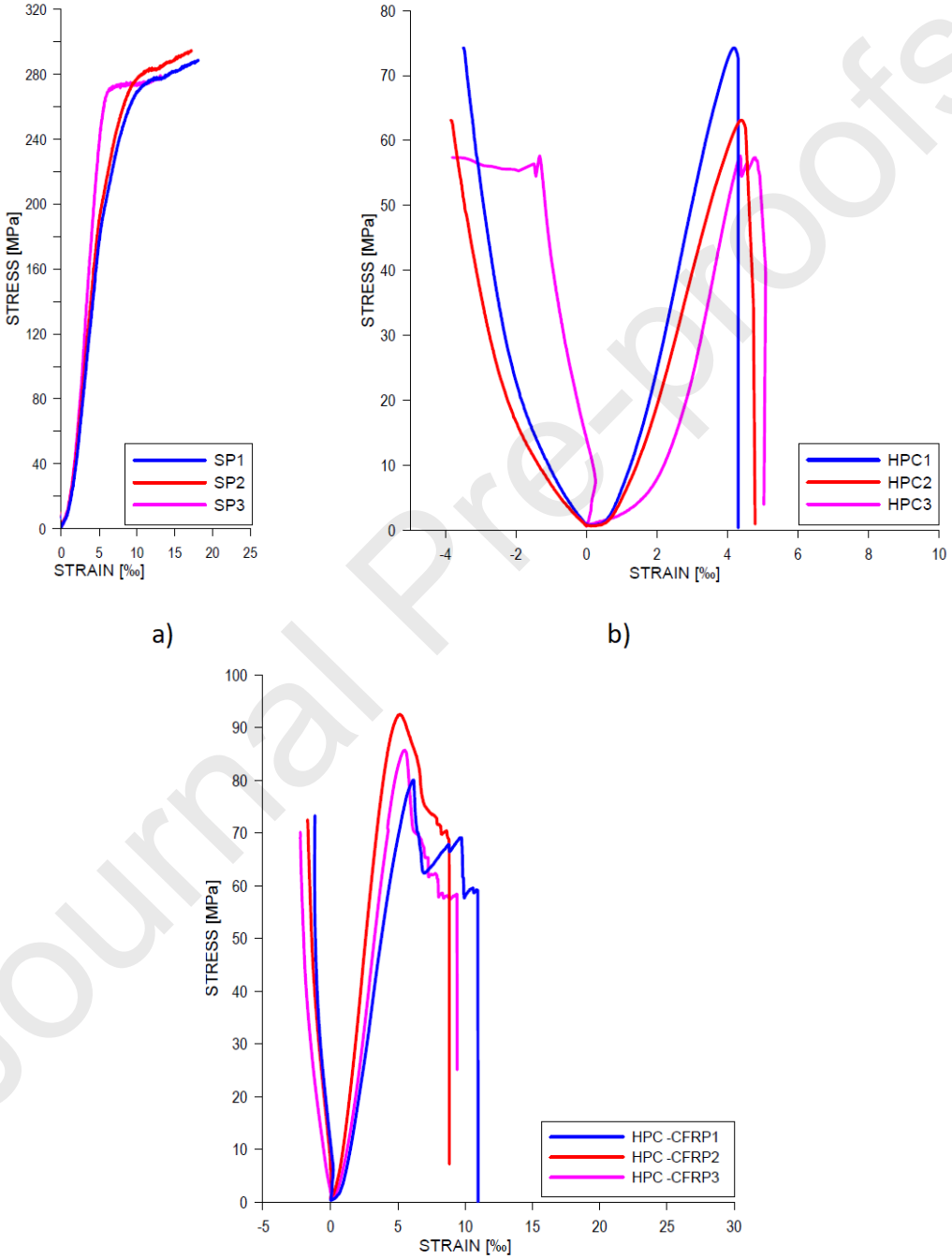

a) b)

c)

Figure 4. Axial stress-strain relationship for: a) steel pipes (SP), b) high performance concrete (HPC), c) high-performance concrete cores reinforced by one layer of carbon fiber-reinforced polymer (HPC-CFRP) specimens

It is widely known that ultimate capacity and ductility are two primary evaluation criterions for structures. The axial stress-strain relationship for hybrid elements is shown in Figure 5. The behaviour of the CFT columns could be described as quasi linear until reaching the maximum stresses, with a tight area of quasiplastic surrounding point 1 (Figure 5a). The further behaviour of the CFT samples can be described as brittle plastic, particularly in the 1-2 and plastic areas, and as plastic after the transitional zone. Connecting the HPC with the steel tube enables a higher load capacity to be obtained and a safer behaviour of elements when compared to the HPC columns. The average compressive strength of the CFT columns is 104.95 MPa, which is 62% higher than that of the HPC. A greater stability of sample behaviour and a much greater deformability (regarding axial strain) of the CFT columns was noticed.

The stress-strain behaviour for the CFCT columns with 1, 2 and 3 layers of CFRP reinforcement is shown in Figure 5b-d, respectively. In the case of the CFCT1 group of specimens, the strain stress curves are similar to those of the CFT columns with the proviso that the behaviour in the case of the CFCT reinforced by 1 layer of CFRP in the post damage range could also be named brittle-plastic behaviour, albeit with a leaping loss of loading capacity caused by the destructive layers of the CFRP confinement. Therefore, this post-peak behaviour is more fragile in its form than in the CFT columns. The average compressive strength for the CFCT1 columns is 115.64 MPa, which is 10% higher than for the CFT columns.

The number of reinforcement layers has a significant effect on the stress strain behaviour of the confined CFCT specimens. In general, the performance characteristics of the CFCT elements are quite similar, depending on the number of reinforcement layers. However, along with the increase in the number of reinforcement layers, the maximum strength of the samples also increases. Moreover, in the case of the CFCT specimens reinforced by 1 layer of CFRP, strengthening was not observed. It is only when samples 2 and 3 are reinforced with composite layers that a significant part of the reinforcement can be seen in the entire stress-strain characteristics. This strengthening uniquely determines the moment of transferring loads to the CFRP reinforcement, thanks to which the module of this reinforcement can be determined. The value of maximum and final deformations also increases after the destruction of the CFRP layers - ε_u. The transition zone, in all of these cases, has a similar course in which the cracking of successive reinforcement layers causes a more or less sudden decrease in the compressive stresses in the samples. The energy of destruction, understood as a field under the stress-strain curves until reaching the maximum load capacity, increases with an increasing number of CFRP layers. As the strength of the samples increases, more rapid cracking and more broken CFRP fibers were observed in the transitional zone. The increase of lateral deformations is proportional to the longitudinal deformation of the analyzed CFCT samples. The average values of axial

deformations for the CFCT samples reinforced with 1, 2 and 3 composite layers are respectively 33%, 109% and 135% higher, than for the CFT columns. The CFCT samples are characterized by the highest load-bearing capacity and deformability of all the samples subjected to destructive testing. Strengthening of the CFCT columns using CFRP mats also increases their stiffness.

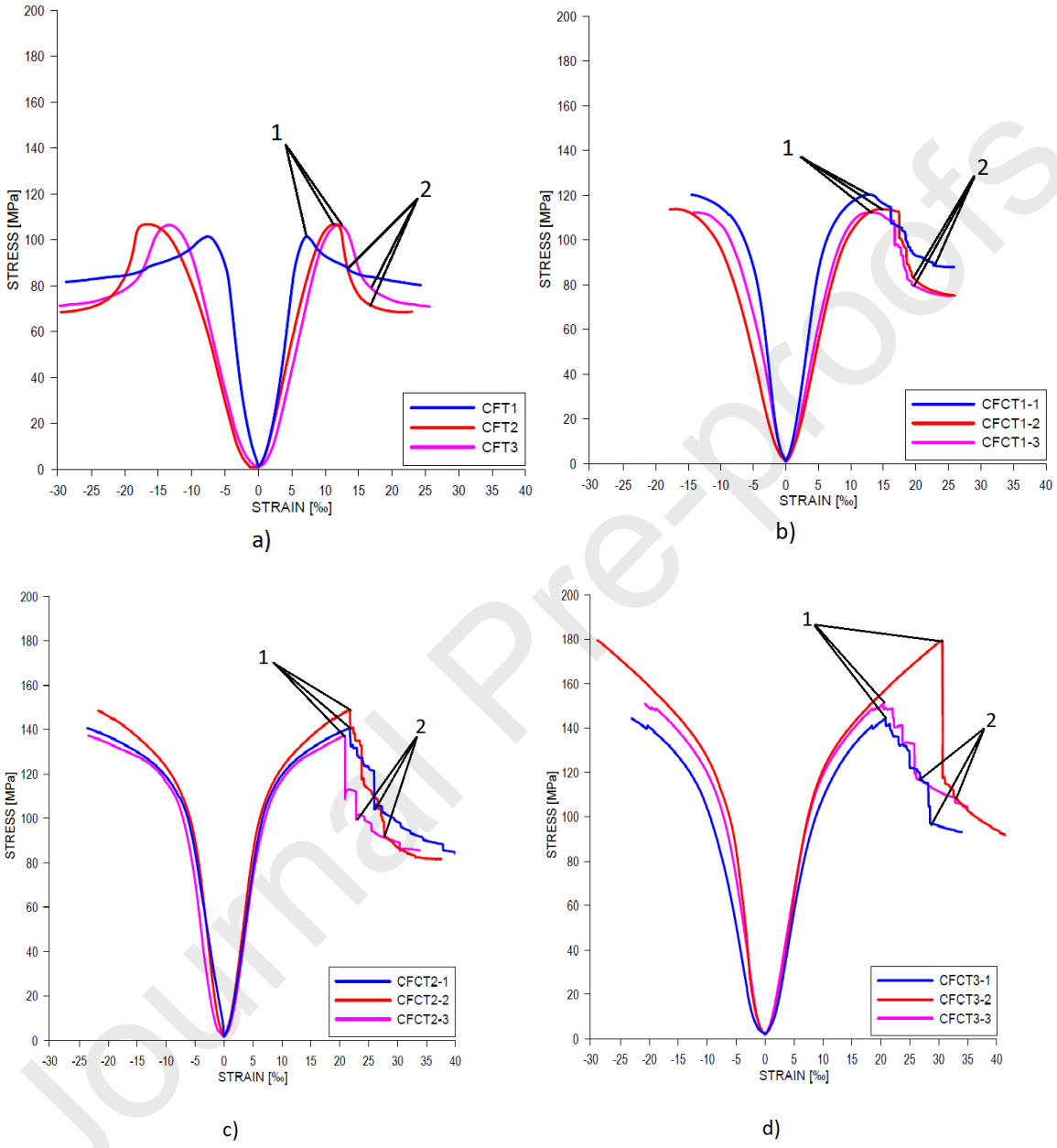

Figure 5. Axial stress-strain relationship for: (a) the concrete-filled steel columns (CFT), (b-d) concrete-filled carbon fiber-reinforced polymer steel composite tubes (CFCT)

4. Numerical analysis

4.1. Numerical model

The crushing simulations were performed using Abaqus software based on the finite element method. For the calculations, the authors used an explicit module of the software and performed nonlinear analyses. The 3D model consisted of four parts (Fig 6a), which were the HPC core, steel tube and from one to three layers of the CFRP, with the last part of the model being a plate, through which the loading, as a displacement, was applied on the top of the column. The bottom of the model was fixed. Figure 6b shows the finite element mesh of the CFCT model.

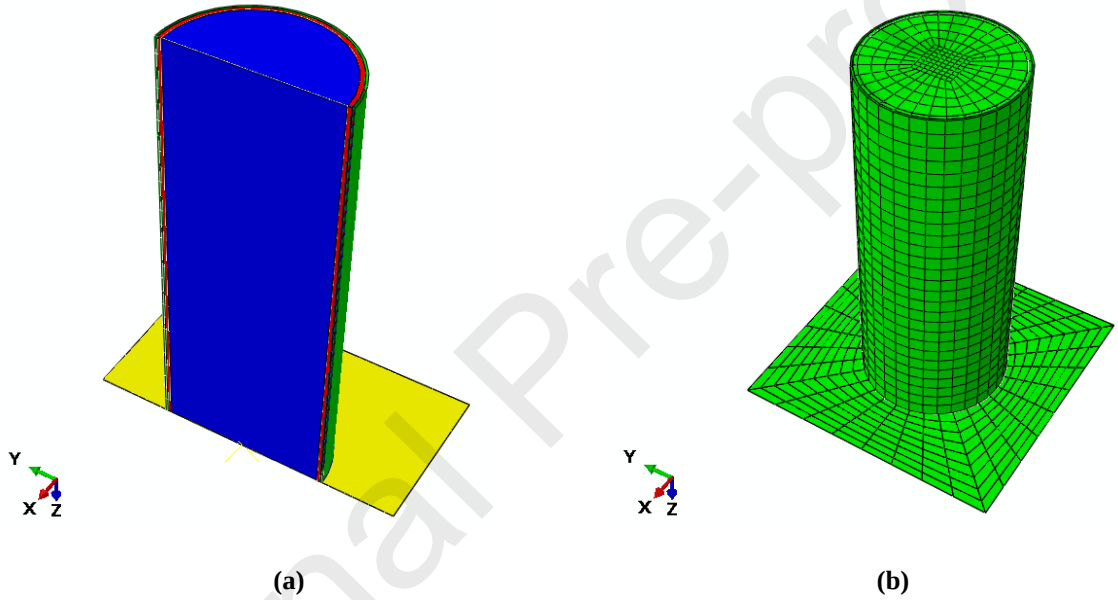

(a) **(b)**

Figure 6. Visualization of the concrete-filled carbon fiber-reinforced polymer steel composite tubes (CFCT) 3D model: (a) model with finite element mesh, (b) 3D model cross-section presenting component parts (blue – HPC; red – steel tube; green – CFRP; yellow – rigid body)

The mentioned plate is defined in the finite element (FE) model as a rigid body that is related with the reference point and located in the central point on the top surface of the 3D model. The load was applied by moving the reference point from the starting position. The concrete column was modeled using eight-node solid hexahedral elements in a three-dimensional state of stress. The HPC model consisted of 10,000 elements. The dimensions of the model were the same as for the samples. The steel tube was modeled as a solid element and consisted of 2500 eight-node hexahedral elements in a three-dimensional state of stress. The dimensions of the steel tube model were the same as in reality. The CFRP was modeled as a deformable solid shell and consisted of 2500 four-node elements. A

single layer of it had the same height as a concrete column and steel tube, which is 400 mm. The thickness of the single layer, which was adopted for the calculations, was 0.167 mm. Layering of the CFRP (in cases which consist of two or three layers) was performed using a composite layup function in Abaqus software. This function allows more than one layer of lamina to be connected without using additional constrains between the contact surfaces.

The aim of the finite element analysis of all the specimens was to observe the buckling, deformed shapes and stress values at the same amount of displacement as for the experimental results (strain controlled model). It should be noted that the proposed type of element that was subjected to the experimental analyses is still not a well-known solution. The numerical modelling aimed at recreating the laboratory tests, and was carried out to better exemplify the behaviour of these types of elements. Moreover, the numerical simulations were carried out to show that modelling of these types of elements is possible and that it reflects reality as much as possible (real structural element/laboratory experiments). This also shows that the proposed methodology can be successfully used in simulations of larger structures or real building structures. It should be noted that in the paper there is only an introduction to testing on larger structural elements, but the main goal, however, was to learn the characteristics and behaviour of the proposed solution, which is the CFCT element. This study shows that CFCT elements will be innovative and effective structural systems in related areas of structural engineering. However, the analysis of the behavior of individual real-scaled beams, frames, and the connections of structural elements should be carried out in order to accurately understand the phenomena that occur in CFCR type elements on a real scale.

4.2. Numerical simulation

To simulate the contact between the steel tube and concrete column, general contact properties were applied. Contact properties consist of friction and normal behaviour between contact surfaces. Between the CFRP and the steel tube, the contact properties were also applied. The authors, in order to simplify the model (because of the large number of parameters of the traction-separation damage model), used tie constraints between the contact surfaces. The performed works were divided into two parts. As is already known, the success of calculations depends on the correct selection of input parameters. The parameters of each part of the model were estimated and separate simulations of the all model parts were performed. The final properties of the materials properties are summarized in Table 7. All the performed simulations were carried out in the same way. The calculations involve dynamic analysis. Due the fact that the authors consider the traced inelastic, unstable, collapse and post buckling behaviour to be a nonlinear problem, the dynamic explicit procedure was chosen as a solution.

Table 7. Basic parameters of the 3D model

High performance concrete (HPC)		Steel		Carbon fiber-reinforced polymer (CFRP)	
Elastic modulus E_c	36 GPa	Elastic modulus E_c	205 GPa	Elastic modulus E_f	230 GPa
Poisson ratio ν_c	0.3	Poisson ratio ν_s	0.3	Poisson ratio ν_f	0.3
Yeld stress σ_{cY}	22.5 MPa	Yeld stress σ_{sY}	235 MPa	Longitudinal tensile strength of the CFRP	4900 MPa
Crushing failure stress σ_{cU}	65 MPa	Ultimate stress σ_{sU}	410 MPa	Transversal tensile strength of the CFRP	217 MPa
Plastic strain at failure ε_{cF}	0.0039			Longitudinal compressive strength of the CFRP	2580 MPa
Cracking failure stress σ_{cT}	2.68 MPa			Transversal compressive strength of the CFRP	64.5 MPa
				Longitudinal shear strength of the CFRP	155 MPa
				Transversal shear strength of the CFRP	155 MPa

4.3. Results of the numerical analysis

At the beginning, the parameters of the HPC were determined. As a constitutive model, the concrete damage plasticity model was used [41], while the elastic behaviour was modelled as isotropic and linear. In this constitutive concrete model, when determining the in-elastic phase of the concrete work, the cooperation of two mechanisms led to the exhaustion of the material load - and thus its destruction

- degradation of the material (represented by the degradation of its rigidity - stiffness degradation) and plasticization. As the maximum compressive strength, the average value of three samples from the laboratory test was adopted for the simulation.

Next, the physical-mechanical parameters of the steel tube were estimated. As a constitutive model of the steel pipe, the elastic-plastic material with isotropic hardening was chosen. In this model, the yield surface is defined using uniaxial stress and corresponds with the value of plastic strain. As input parameters, the average values of the laboratory tests (true values of stress and strain) were adopted for the calculations. The results of the simulation have been presented in graph form as a strain-stress curve. The next step of calculations was to perform analysis for the CFT sample. In this case, the parameters from the calibration of the steel and HPC models were used (Table 7). The procedure of the calculations was the same as earlier. As was mentioned before, the general contact properties were applied (friction and normal behaviour) between the contact surfaces of the steel and concrete section.

The physical-mechanical properties of the CFRP lamina was determined theoretically due to the fact that a laboratory test was not performed in this study. As a constitutive model, the Hashin Damage model for fiber-reinforced composite was chosen [42]. In this model, a series of damage parameters need to be defined, including longitudinal and transverse tensile strength, longitudinal and transverse compressive strength, and longitudinal and transverse shear strength. The way of estimating these properties (including the approach of different authors) is shown e.g. in [43]. The idea of determining the physical-mechanical parameters is based on the micromechanical approach. In the simulation of the HPC-CFRP sample, the physical-mechanical properties of the CFRP lamina, which were estimated theoretically, and the concrete parameters from the HPC model calibration were used (Table 7). As already mentioned, the CFRP lamina was modeled as a composite layup. The contact surfaces between the CFRP lamina and the concrete were constrained using a tie constrain. The last stage of the finite element analyses was to perform calculations for the CFCT specimens with one, two and three layers of CFRP lamina. As before, the CFRP lamina was again modeled as a composite layup with physical-mechanical parameters. The contact between the CFRP and steel tube surfaces was executed as a tie constrain, while the connection between the steel tube was based on general contact with frictional (friction coefficient) and normal behaviour (hard contact).

The results of the simulation are presented as a strain-stress curve in Figure 7 and compared with the results from the laboratory test.

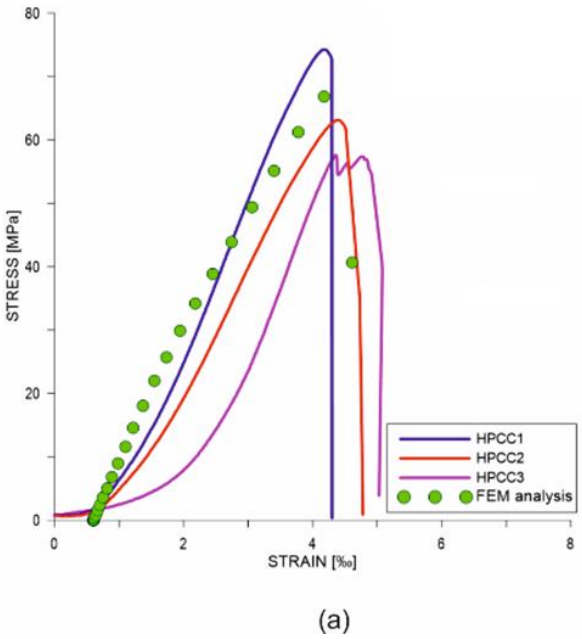

(a)

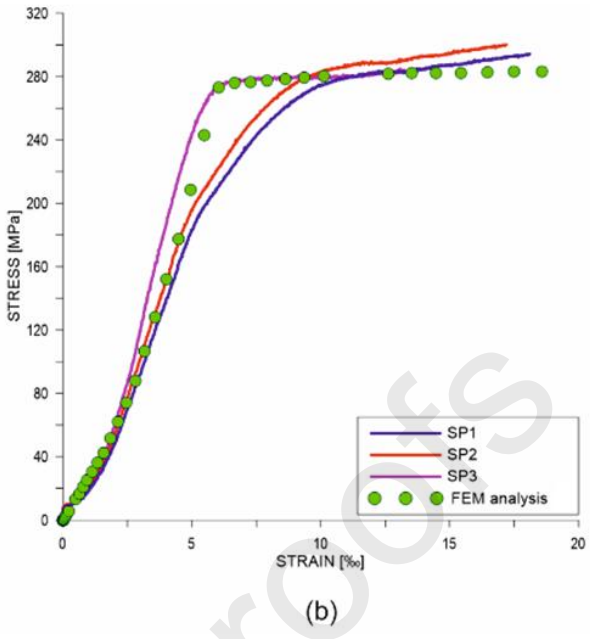

(b)

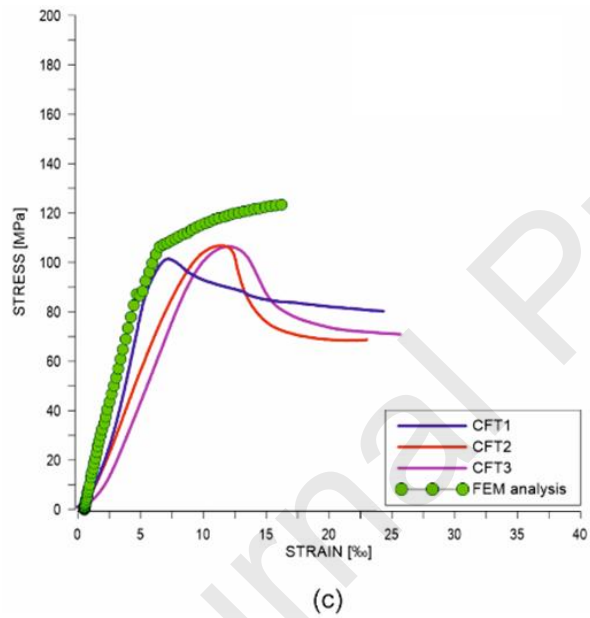

(c)

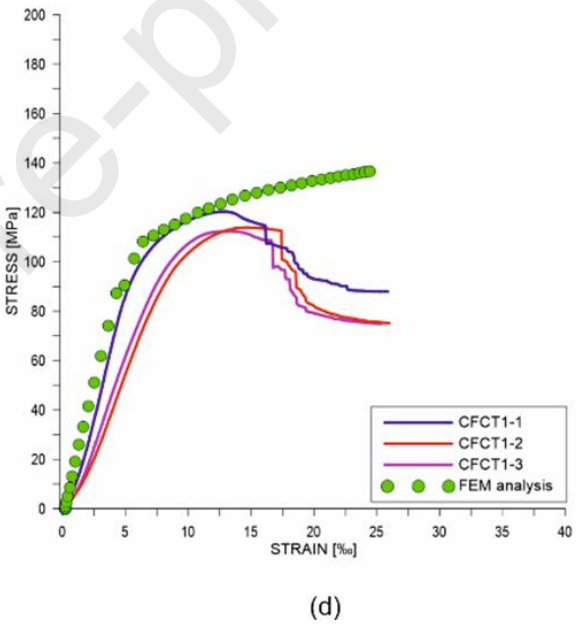

(d)

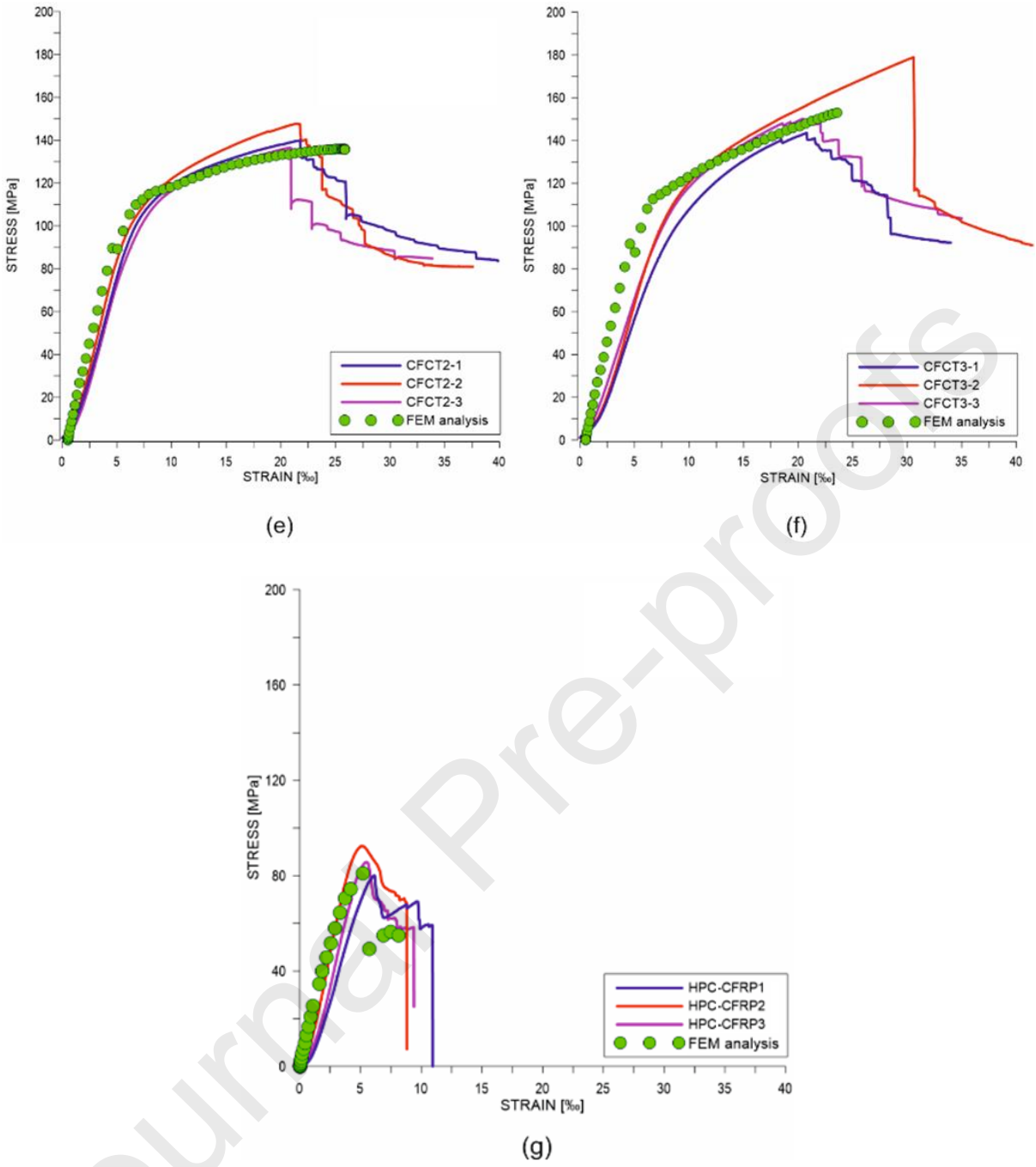

Figure 7. Compared results of FEM analysis with those of the laboratory test for each group of specimens: (a) HPC, (b) steel pipe (SP), (c) concrete-filled steel columns (CFT), (d) CFCT 1, (e) CFCT 2, (f) CFCT 3, (g) HPC-CFRP

As can be seen in the figures, the course of the stress-strain function obtained as a result of numerical analysis qualitatively corresponds to the results of the laboratory tests. The resulting discrepancies between the laboratory tests and the numerical simulations appear as a result of the adoption of the average parameters from the three laboratory tests for the individual materials (HPC, steel, CFRP). Taking this into account and the fact that the constitutive model of the steel was the ideal plastic

isotropic model, the resulting model of the CFCT sample and the simulation results should be taken as qualitatively reflecting reality.

The article presents an analysis of the behaviour of 400 mm high samples, i.e. relatively short columns (L/D <3). However, it should be noted that the carried out research is preliminary to further considerations in this field. Laboratory tests of elements with a larger L/D ratio will be conducted in order to be able to relate the known properties of the CFCT elements to e.g. real scaled column beam capacities, frames etc. Initial tests on larger elements have already been conducted, among others by Kim et al. [44], and give a small view on how such elements will behave at an L/D ratio greater than 3. The authors conducted tests for samples with a slenderness ratio of 7.8 and 11.8. Research shows that the strength of CFRP columns filled with concrete decreases as the L/D ratio increases. Bourouz also came to similar conclusions [45]. In his paper, he included the comparison of results recorded from wrapped RC specimens that have an equal cross section. The results show that the increase of the slenderness ratio, within the range of values from 2 to 7, generally leads to a small decrease in the load carrying capacity and a moderate reduction in the axial deformation. Similar conclusions were presented, among others, by Etman [46] in an article on strengthening RC columns with different slenderness ratios using "CFRP" wraps; by Elsanadedy [47] in numerical investigations of the size effects in CFRP-wrapped concrete columns; by Jiang and Wu [48] in experiments on concrete-filled CFRP–PVC columns; and by Soliman [49] who investigated concrete columns wrapped with CFRP.

5. Conclusions and perspectives

This work presents an experimental investigation of the compressive behaviour of steel tubes filled with high performance concrete confined by a various number of carbon fiber-reinforced polymer (CFRP) jackets. The following conclusions can be drawn from the work presented in the paper:

- The number of reinforcement layers significantly affects the stress strain behaviour of concrete-filled carbon fiber-reinforced polymer steel composite tubes (CFCT) specimens. In general, the performance characteristics of CFCT elements are quite similar in their essence, depending on the number of reinforcement layers. However, along with the increase in the number of reinforcement layers, the maximum strength of the samples also increases.
- The presented results show that the energy of destruction, understood as a field under the stress-strain curves until reaching the maximum load capacity, increases with an increasing number of CFRP layers. As the strength of the samples increases, there are more rapid cracking in the transitional zone and more broken CFRP fibers are observed. The observed increase of lateral deformations was proportional to the longitudinal deformation of the analyzed CFCT samples.
- It was shown that in the case of high performance concrete (HPC), the stress–strain curves of the confined specimens can be divided into two distinct regions. The stress-strain behaviour

of confined CFRP was similar to that reported in the literature. These regions include the elastic stage involved with the transfer of stresses by the CFT, and also the hardening stage, where stresses are carried by the CFRP confinement, which provides the columns with post-yield stiffness for load carrying.

- The confined specimens fail because of rupture of the CFRP in the region of weakness. After reaching the maximum strain, fragile-plastic behaviour of the specimens with a leaping loss of stiffness can be observed.
- The carried out numerical calculations are based on the average values of the physical-mechanical parameters obtained from the laboratory tests. Qualitatively, the results of the numerical simulations correspond to those obtained in the laboratory tests.
- The probable reason for the invisible destruction of the CFCT sample in the stress-strain diagrams is due to the insufficient number of post-parameters for the calculations.

The results presented in the article are a first step in fully characterizing the compressive behaviour of concrete-filled carbon fiber-reinforced polymer steel composite tube columns made of high performance concrete. In the authors' opinion, future studies should concentrate on testing the practical dimensions of such dimension columns.

Acknowledgements

The author would like to thank D.Sc. PhD. Eng. Jerzy Cieślik for his help and experience when performing the compressive tests. The authors would also like to thank M.Sc. Eng. Marek Kawalec form SIKA Poland for technical support and the composite materials.

References:

1. Yang W, Gang W, Guofen L. Performance of circular concrete-filled fiber-reinforced polymer-steel composite tube columns under axial compression. J Reinf Plast Comp 2014;33(20):1911–1928.
2. O'Shea MD, Bridge RQ. Design of circular thin-walled concrete filled steel tubes. J Struct Eng ASCE 2000;126:1295–1303.
3. Gardner NJ, Jacobson ER. Structural behavior of concrete filled steel tubes. ACI J Proc 1967;64:404–413.
4. Jizhong W, Lu Ch, Junlong Y. Compressive behavior of CFRP-steel composite tubed steel-reinforced columns with high-strength concrete. J Constr Steel Research 2018;150:354–370.

5. Ostrowski K. The influence of CFRP sheets on the strength of specimens produced using normal concrete and high-performance concrete assessed using uniaxial compression tests. Technical Transaction 2017;7(114):41-51.
6. Mayer P, Kaczmar J. Właściwości i zastosowania włókien węglowych i szklanych. Tworzywa Sztuczne i Chemia 2008;6:50-55.
7. Trapko T. The effect of high temperature on the performance of CFRP and FRCM confined concrete elements. Compos Part B 2013,54:138–145.
8. Ostrowski K, Kinasz R, Cieślik J, Wałach D. The influence of CFRP sheets on strength of short columns produced from normal strength concrete and fibre rein-forced concrete. Technical Transaction. Civil Engineering 2016;113(2-B):145-156.
9. Lim JC, Ozbakkaloglu T. Confinement model for FRP-confined high-strength concrete. Journal of Composites for Construction 2013;18(4).
10. Jiang S, Fernando D, Ho JCM, Heitzmann M. Behavior of FRP confined ultrahighstrength concrete columns under axial compression: An experimental study. In: Mechanics of Structures and Materials: Advancements and Challenges, Proceedings of the 24th Australasian Conference on the Mechanics of Structures and Materials (ACMSM/24), Perth,WA, 6-9 December 2016. p. 1737-1744.
11. Chikh N, Gahmous M, Benzaid R. Structural Performance of High Strength Concrete Columns Confined with CFRP Sheets. Proceedings of the World Congress on Engineering, London, U. K., 4-6 July 2012.
12. Kaminski M, Trapko T. Experimental behavior of reinforced concrete column models strengthened by CFRP materials. J Civ Eng Manage 2006;12(2):109–115.
13. Berthet JF, Ferrier E, Hamelin P. Compressive behaviour of concrete externally confined by composite jackets. Part A: experimental study. Construction and Building Materials 2005;19(3):223-232.
14. Park TW, Na UJ, Chung L, Feng MQ. Compressive behavior of concrete cylinders confined by narrow strips of CFRP with spacing. Composites: Part B 2008;39(7–8):1093–103.
15. Campione G, Miraglia N. Strength and strain capacities of concrete compression members reinforced with FRP. Cement Concr Compos 2003;25(1):31–41.
16. Koosha K, Pedram S. Performance of high-modulus near-surface-mounted FRP laminates for strengthening of concrete columns. Composites: Part B 2019;164:90-102.
17. Rajai Z, Al-Rousan, Muneer HB. Impact of curvature type on the behaviour of slender reinforced concrete rectangular column confined with CFRP composite. Composites: Part B 2019;173:106939.
18. Mohammed AZ, Hayder AR, Alkhrdaji T. Performance of CFRP-strengthened concrete beams fastened with distributed CFRP dowel and fiber anchors. Composites: Part B 2019; in press, accepted manuscript.

19. Huifeng Zhang, Jin Wu, Fengyu Jin, Chengjun Zhang. Effect of corroded tension reinforcements on flexural performance of reinforced recycled aggregate concrete beams strengthened with CFRP. Composites: Part B 2019;162: 589-599.
20. Sadrmomtazi A, Khabaznia M, Tahmouresi B. Effect of Organic and Inorganic Matrix on the Behavior of FRP-Wrapped Concrete Cylinders. Journal of Rehabilitation in Civil Engineering 2016;4(2):52-66.
21. Colajanni P, De Domenico F, Recupero A, Spinella N. Concrete columns confined with fibre reinforced cementitious mortars: experimentation and modelling. Construction and Building Materials 2014;52:375-384.
22. Ozbakkaloglu T. Behavior of square and rectangular ultra high-strength concrete-filled FRP tubes under axial compression. Compos Part B Eng 2013;54:97–111.
23. Ozbakkaloglu T. Compressive behavior of concrete-filled FRP tube columns: Assessment of critical column parameters. Eng Struct 2013;51:188–199.
24. Ozbakkaloglu T. Axial compressive behavior of square and rectangular high-strength concrete-filled FRP tubes. J Compos Constr 2013;17:151–161.
25. Fam A, Manda S and Rizkalla S. Rectangular filament wound glass fiber reinforced polymer tubes filled with concrete under flexural and axial loading: Analytical modelling. J Compos Constr 2005;9:34–43.
26. Zhu ZY, Ahmad I, Mirmiran A. Seismic performance of concrete-filled FRP tube columns for bridge substructure. J Bridge Eng 2006;11:359–370.
27. Karimi K, Tait MJ, El-Dakhakhni WW. Influence of slenderness on the behaviour of a FRP-encased steel concrete composite column. J Compos Constr 2012;16:100–109.
28. Karimi K, Tait MJ, El-Dakhakhni WW. Analytical modelling and axial load design of a novel FRP-encased steel-concrete composite column for various slenderness ratios. Eng Struct 2013;46:526–534.
29. Huang L, Gao C, Yan L, Yu T, Kasal B. Experimental and numerical studies of CFRP tube and steel spiral dual-confined concrete composite columns under axial impact loading. Composites Part B: Engineering 2018;152:193-208.
30. Xiao Y, He WH, Choi KK. Confined concrete-filled tubular columns. J Struct Eng ASCE 2005;131:488–497.
31. Liu L, Lu YY. Axial bearing capacity of short FRP confined concrete-filled steel tubular columns. J Wuhan Univ Technol 2010;25:454–458.
32. Hu YM, Yu T, Teng JG. FRP-confined circular concrete-filled thin steel tubes under axial compression. J Compos Constr 2011;15:850–860.
33. Park JW, Hong YK, Hong GS, Kim JH. Design formulas of concrete filled circular steel tubes reinforced by carbon fiber reinforced plastic sheets. Procedia Eng 2011;14:2916–2922.

34. Prabhu GG, Sundarraja MC. Behaviour of concrete filled steel tubular (CFST) short columns externally reinforced using CFRP strips composite. Constr Build Mater 2013;47:1362–1371.
35. Sundarraja MC, Prabhu GG. Investigation on strengthening of CFST members under compression using CFRP composites. J Reinf Plast Compos 2011;30:1251–1264.
36. Teng JG, Hu YM, Yu T. Stress-strain model for concrete in FRP-confined steel tubular columns. Eng Struct 2013;49:156–167.
37. Smith, ST, Kim MSJ, Zhang HW. Behaviour and Effectiveness of FRP Wrap in the Confinement of Large Concrete Cylinders. J. Compos. Constr. 2010;14:573–582.
38. Yiyan L, Na L, Shan L. Behaviour of FRP-Confined Concrete-Filled Steel Tube Columns. Polymers 2014;6(5):1333-1349
39. EN 206:2013, Concrete – Specification, performance, production and conformity.
40. EN 12390-3:2009, Testing Hardened Concrete. Compressive Strength of Test Specimens; Polish Committee for Standardization: Warszawa, Poland, 2009.
41. Lubliner J, Oliver J, Oller S, Onate E. A plastic-damage model for concrete. International Journal of Solids and Structures1989;25(3):299-326
42. Hashin Z. Failure criteria for unidirectional fibre composites. ASME Journal of Applied Mechanics 1980;47(2):329-334.
43. Lupăşteanu V, Ţăranu N, Popoaei S. Theoretical Strength Properties of Unidirectional Reinforced Fiber Reinforced Polymer Composites. Bulletin of the Polytechnic Institute of Jassy 2013;63(6):83-98.
44. Kim H, Suntharavadivel TG, Duan K. Experimental Study of Concrete Filled FRP Tubes under Axial Loading. 5th International Conference on Sustainable Built Environment. Kandy, Srilanka. 2014;1-6.
45. Bourouz A, Chikh N, Benzaid R, Laraba A. Confinement of High Strength Concrete Columns with CFRP Sheets. Proceedings of the World Congress on Engineering. London, UK. 2014
46. Etman EE. Efficiency of strengthening R C columns, with different slenderness ratios, using "CFRP" wraps. 27th Conference on OUR WORLD IN CONCRETE & STRUCTURES. Singapore, 2002.
47. Elsanadedy HM, Al-Salloum YA, Alsayed SH, Iqbal RA. Experimental and numerical investigation of size effects in FRP-wrapped concrete columns. Construction and Building Materials. 2012;29:56-72
48. Jiang SF, Ma SL, Wu ZQ. Experimental study and theoretical analysis on slender concrete-filled CFRP–PVC tubular columns. Construction and Building Materials. 2014;53:475-487
49. Soliman AES. Behaviour of long confined concrete column. Ain Shams Engineering Journal. 2011;2(3-4):141-148